
Archiv-Ex.:

FZR-39

May 1994

Preprint

W. Iskra, M. Müller and I. Rotter

Radial pattern
of nuclear decay processes

Radial pattern of nuclear decay processes

W. Iskra^{1,2}, M. Müller¹ and I. Rotter^{1,3}

¹ *Forschungszentrum Rossendorf, Institut für Kern- und Hadronenphysik,
D-01314 Dresden, Germany*

² *Soltan Institute for Nuclear Studies, PL-00-681 Warszawa, Poland*

³ *Technische Universität Dresden, Institut für Theoretische Physik,
D-01062 Dresden, Germany*

Abstract

At high level density of nuclear states, a separation of different time scales is observed (trapping effect). We calculate the radial profile of partial widths in the framework of the continuum shell model for some 1^- resonances with $2p-2h$ nuclear structure in ^{16}O as a function of the coupling strength to the continuum. A correlation between the lifetime of a nuclear state and the radial profile of the corresponding decay process is observed. We conclude from our numerical results that the trapping effect creates structures in space and time characterized by a small radial extension and a short lifetime.

1

Recently, the properties of open quantum systems are investigated in the framework of different models [1 - 12]. In most cases studied, the number N of resonance states is much larger than the number K of open decay channels. One of the results obtained is the *trapping effect* which appears if the average width $\bar{\Gamma}$ of the resonance states is of the same order of magnitude as their average distance \bar{D} . In this case, a redistribution takes place inside the nucleus which results in the formation of K short-lived resonance states ("broad states") together with $N - K$ long-lived ones ("narrow states"). The time-scales of both types of states are well separated from each other.

The trapping effect is shown to occur in realistic many-body quantum systems such as nuclei [4]. Here, at low level density, the nuclear spectroscopic properties are relevant, while at higher level density, the properties of nuclei are described well by the unified theory of nuclear reactions where the open decay channels are relevant. It is exactly this transition which is described by the redistribution taking place inside the nucleus at the critical degree $\bar{\Gamma}/\bar{D} \approx 1$ of resonance overlapping.

Further, the trapping effect explains the different properties of resonances observed in light and heavy nuclei. While the lifetimes of the resonances in light nuclei are of the order of magnitude of the collision time between nucleons (apart from selection rules), the resonances in heavy nuclei are very long-lived. They are strongly mixed in the basic shell-model wavefunctions what corresponds to the original definition of the compound nucleus given by Bohr [13].

The trapping effect is the result of the interference between a certain number N of overlapping resonances. Thus, one could expect that the radial extensions of the broad and narrow states are of comparable size. On the other hand, the lifetimes of the long-lived and short-lived states differ strongly from each other so that there exists, maybe, a correlation with the radial extension of the nucleus.

There are two different possibilities for such a correlation which both have their own justification. One could imagine that the long-lived states have a narrower radial extension than the short-lived ones with the consequence that they are screened from the continuum. This might be the reason for their long lifetimes. Another idea is the interpretation of the trapping effect as the formation of "structures in space and time" by selforganization [14].

In such a case, the radial extension of the short-lived states is expected to be smaller than that of the long-lived ones. In this case, the broad states appear to be localized in both time and space while the long-lived states are spread over a larger extension in time as well as in space.

The purpose of our investigation is to clarify whether there is any relation between the lifetimes of resonance states and their radial extension. In our calculations, the radial extension of a state is *not* determined directly. We calculate, instead, the radial pattern of the partial width amplitudes, i.e. of the area at which the emission of the particles from the resonance states takes place. The partial width amplitudes vanish at the centre of the nuclear states where the channel wavefunctions are small, and are sensitive to the radius of the resonance state where its wavefunction vanishes. The results obtained show clearly a correlation between lifetime and radius of different states.

2

The radial profile of the partial width amplitudes is studied in the framework of the continuum shell model in line with the method described in [15].

In the continuum shell model, the Schrödinger equation

$$(H - E)\Psi = 0 \tag{1}$$

is solved with an ansatz containing both bound and unbound states. The total function space is subdivided, by using the projector operator technique, into the two orthogonal subspaces P and Q under the condition $P + Q = 1$. The subspace Q contains the many-body states of A nucleons formed by the antisymmetrized products of the wavefunctions of the single-particle bound states and of the single-particle resonance wavefunctions up to some cut-off radius. Therefore, the structural part in the continuum shell model is the same as in the standard shell-model approaches. The eigenstates Φ_R^{SM} of the Q -projected Hamiltonian H_{QQ} are called [16] "quasibound states embedded in the continuum" (QBSEC). These QBSEC's differ from the "bound states embedded in the continuum" (BSEC) introduced by Mahaux and Weidenmüller [17] by the contribution of the single-particle resonances from the interior of the nucleus ("cut-off procedure"). The subspace P contains the many-body states with $A - 1$ nucleons in bound orbits and one nucleon in a scattering state as well as the part of the single-particle resonance wavefunc-

tions beyond the cut-off radius.

Using the cut-off procedure for single-particle resonances, it is possible to identify the matrix elements

$$\begin{aligned}\tilde{\gamma}_{Rc} &= (2\pi)^{1/2} \langle \tilde{\Omega}_R | V | \chi_E^c \rangle \\ &= (2\pi)^{1/2} \langle \tilde{\Phi}_R | V | \xi_E^c \rangle\end{aligned}\quad (2)$$

with the amplitudes of the partial widths [18]. Here, the $\tilde{\Phi}_R$ are the eigenfunctions of the non-Hermitian operator

$$H_{QQ}^{eff} = H_{QQ} + H_{QP} G_P^{(+)} H_{PQ} \quad (3)$$

where $G_P^{(+)}$ is the Green function in the P -subspace and

$$H = H_0 + V \quad (4)$$

contains the central potential H_0 as well as the two-particle residual interaction V . Using the projector operator formalism, the Hamiltonian consists of four parts

$$H = H_{QQ} + H_{QP} + H_{PQ} + H_{PP} \quad (5)$$

where $H_{PQ} \equiv PHQ$ and so on. It is $\tilde{\Phi}_R = \sum_{R'} a_{RR'} \Phi_{R'}^{SM}$ with complex coefficients $a_{RR'}$. The functions ξ_E^c are solutions of the coupled channel equations $(H_{PP} - E)\xi_E^c = 0$ while the χ_E^c are the channel wavefunctions (wavefunctions of the target nucleus in a certain state and one unbound nucleon). The functions

$$\tilde{\Omega}_R = (Q + G_P^{(+)} H_{PQ}) \tilde{\Phi}_R \quad (6)$$

are the wavefunctions of the resonance states R . The details of the model can be found in [16, 4].

According to the method used in [15], the radial profile of the amplitudes of the partial widths is calculated from

$$\tilde{\gamma}_{Rc}^r = (2\pi)^{1/2} \langle \tilde{\Phi}_R | V \delta(r - r') | \xi_E^c \rangle \quad (7)$$

where $\delta(r - r')$ is the Dirac delta function. An integration over the radius variable r' in the matrix elements gives us the r -dependent characteristics.

The calculations are performed for different values

$$\begin{aligned} W^{ex} &= \langle \Phi_{R'}^{SM} | H_{QP} G_P^{(+)} H_{PQ} | \Phi_R^{SM} \rangle \\ &= \langle \Phi_{R'}^{SM} | V^{ex} G_P^{(+)} V^{ex} | \Phi_R^{SM} \rangle \end{aligned} \quad (8)$$

of the mixing of two resonance states via the continuum of decay channels ("external mixing"). For this purpose, the external part $V^{ex} = \alpha^{ex} V$ of the interaction in H_{PQ} , H_{QP} and H_{PP} is varied by means of varying the parameter α^{ex} . The internal part $V^{in} = \alpha^{in} V$ of the interaction between bound states appearing in H_{QQ} remains constant in our calculations ($\alpha^{in} = 1$). By varying the external mixing W^{ex} , we change effectively the average degree $\bar{\Gamma}/\bar{D}$ of overlapping of the resonances (Table 1).

3

Some typical results of our calculations are shown in Figs. 1 and 2. We have chosen a configuration space of $N = 70$ states 1^- of ^{16}O with 2p-2h nuclear structure and the $1s$, $1p_{3/2}$, $1p_{1/2}$, $2s$ and $1d_{5/2}$ shells. The number of open decay channels is $K = 2$, which are either the two proton channels $^{15}\text{N}_{3/2^-} + p$ and $^{15}\text{N}_{1/2^-} + p$, (Fig. 2) or the two neutron channels $^{15}\text{O}_{3/2^-} + n$ and $^{15}\text{O}_{1/2^-} + n$ (Fig. 1). The energy of the system is $E = 34$ MeV. The inelastic channel opens at $E = 6.30$ MeV in the proton decay and at $E = 6.15$ MeV in the neutron decay, i.e. there are no threshold effects at the energy considered [12]. The parameters of the Woods-Saxon potential for neutrons as well as for protons are taken from calculations describing proton scattering on ^{15}N [12, 16]. The Coulomb potential corresponds to a homogeneous charged sphere of radius $1.25 \cdot (A - 1)^{1/3} = 3.08$ fm. The parameters of the residual interaction V are the same as in [12].

The calculations are performed for $\alpha^{ex} = .2$ up to $\alpha^{ex} = 8$. The trapping effect appears at $\alpha_{cr}^{ex} \approx 2.6$ where $\bar{\Gamma}/\bar{D} \approx 1$ (see table 1) [12], i.e. our calculations at $\alpha^{ex} = .2$ are well below the critical region α_{cr}^{ex} while those with $\alpha^{ex} = 8$ are beyond it. The widths $\tilde{\Gamma}_R$ of the states are given in table 1. In each case, $R = 1, 2$ are the two states with the largest widths (second and third columns). The sum of the widths of the remaining 68 states as well as its averaged squared deviation χ^2 are given in the two last columns. Just above the critical point α_{cr}^{ex} , where the two broad states separate from the other resonances, the widths of most of the trapped modes decrease. Therefore, the χ^2 show a minimum in this region of α^{ex} .

The wavefunctions $\tilde{\Phi}_R$ and the matrix elements $\tilde{\gamma}_{Rc}$ are complex. In Figs. 1a to 1h, $Re\{\tilde{\gamma}_{Rc}^r\}$ for the inelastic neutron channel is drawn for $\alpha^{ex} = .2$ to 8. In Fig. 2, $Re\{\tilde{\gamma}_{Rc}^r\}$ as well as $Im\{\tilde{\gamma}_{Rc}^r\}$ are shown for both channels c_1 (Figs. 2a,b,e,f) and c_2 (Figs. 2c,d,g,h) in the case of proton decay and for $\alpha^{ex} = .2$ and 8. In any case, the $\tilde{\gamma}_{Rc}^r$ for the two states $R = 1, 2$ with the largest widths are represented by dashed lines while the $\tilde{\gamma}_{Rc}^r$ of all the other states $R = 3, \dots, 70$ are shown by dots at the radii r for which the calculations are performed. The solid curves in Fig. 1 are drawn for a typical trapped state.

The results of our calculations show the following: With increasing α^{ex} the amplitudes $\tilde{\gamma}_{Rc}^r$ increase for all states. Further, the transition matrix elements for the broad states get dominant peaks at small radii if the coupling strength increases although the channel wavefunctions have a small amplitude at small radii. That means, the fast decays take place mostly in the inner part of the nucleus. In contrast to that, the decay of the trapped states is distributed over the whole nucleus.

In other words, most nucleons which appear quickly from the short-lived resonances, are emitted in the internal region. The nucleons emitted in the surface region arise mostly from the long-lived states at a later time. This result is independent of the charge of the emitted particle (compare Figs. 1a, 1h and 2c, 2d). It is well expressed for the calculations with $\alpha^{ex} > \alpha_{cr}^{ex}$ where the widths of the two broadest resonances are well separated from those of the other 68 resonances.

It should be underlined here that the $\tilde{\gamma}_{Rc}^r$ of the two broadest resonances $R = 1, 2$ do not change their sign as a function of r in our calculations for α^{ex} above the critical point. After integrating over r , that leads to large $\tilde{\gamma}_{Rc}$. This is not so, generally, for the other resonances, above all at $\alpha^{ex} > 2.5$ where the resonances $R = 3, \dots, 70$ are trapped.

Another numerical result is that the $\tilde{\gamma}_{Rc}^r$ of the two resonances $R = 1$ and 2 have a similar dependence on r at $\alpha^{ex} = 3 - 8$. This is connected with the channel-channel coupling which is large at large α^{ex} .

Table 1: The main characteristics of the resonance states

α^{ex}	$\bar{\Gamma}/\bar{D}$	$\tilde{\Gamma}_1/MeV$	$\tilde{\Gamma}_2/MeV$	$\sum_{R=3}^{70} \tilde{\Gamma}_R^{tr}/MeV$	$\chi^2(\tilde{\Gamma}^{tr})/MeV$
protons					
.2	0.005	0.01	0.005	0.049	6.5E-05
1.5	0.325	0.66	0.34	2.9	3.4E-03
2.5	0.891	2.4	1.7	6.6	3.8E-02
4	2.212	10.3	9.6	6.7	1.4E-02
8	5.103	43.9	37.2	14.3	2.2E-01
neutrons					
.2	0.006	0.01	0.005	0.049	6.5E-05
1.5	0.322	0.71	0.53	2.6	3.3E-03
2.5	0.881	2.8	2.6	5.2	1.8E-02
4	2.187	10.3	10.0	6.0	8.4E-03
8	5.419	43.2	37.6	14.5	2.3E-01

$$\chi^2(\tilde{\Gamma}^{tr}) = \overline{(\tilde{\Gamma}_R^{tr} - \tilde{\Gamma}_R^{tr})^2}$$

4

Summarizing, we conclude from our results on decaying states that there exists a correlation between the lifetimes of the states and their radial extensions. In the short-time scale, most nucleons are emitted from the regions of small radii. The nucleons emitted from the surface region of the nucleus appear mainly in the long-time scale. That means, we observe a correlation of the decay probability of nuclear states with their radial extension. The shorter the lifetime of a state, the smaller is its radius.

The results of our calculations support, therefore, the assumption that the trapping effect creates "structures in space and time". In this manner, the trapping effect may be considered as a signature for selforganization in the nuclear system.

Acknowledgment: The present investigations are supported by the Deutsche Forschungsgemeinschaft (Ro 922/1) and by the Bundesministerium für Forschung und Technologie (WTZ X081.39).

References

- [1] P. Kleinwächter and I. Rotter, Phys. Rev. C 32, 1742 (1985); I. Rotter, J. Phys. G 12, 1407 (1986); 14, 857 (1988); Fortschr. Phys. 36, 781 (1988)
- [2] V.V. Sokolov and V.G. Zelevinsky, Phys. Lett. B 202, 10 (1988); Nucl. Phys. A 504, 562 (1989)
- [3] V.B. Pavlov-Verevkin, Phys. Lett. A 129, 168 (1988); F. Remacle, M. Munster, V.B. Pavlov-Verevkin and M. Desouter-Lecomte, Phys. Lett. A 145, 265 (1990)
- [4] I. Rotter, Rep. Prog. Phys. 54, 635 (1991) and references therein
- [5] F.M. Dittes, I. Rotter and T.H. Seligman, Phys. Lett. A 158, 14 (1991)
- [6] F.M. Dittes, H.L. Harney and I. Rotter, Phys. Lett. A 153, 451 (1991)

- [7] V.V. Sokolov and V.G. Zelevinsky, *Ann. Phys. (N. Y.)* 216, 323 (1992) and references therein
- [8] F. Haake, F. Izrailev, N. Lehmann, D. Saher and H.J. Sommers, *Z. Phys. B* 88, 359 (1992)
- [9] R.D. Herzberg, P. von Brentano and I. Rotter, *Nucl. Phys. A* 556, 107 (1993)
- [10] W. Iskra, I. Rotter and F.M. Dittes, *Phys. Rev. C* 47, 1086 (1993)
- [11] K. Someda, H. Nakamura and F.H. Mies, *Progr. Theoretical Phys.* (in press)
- [12] W. Iskra, M. Müller and I. Rotter, *J. Phys. G* 19, 2045 (1993)
- [13] N. Bohr, *Nature* 137, 344 (1936)
- [14] I. Prigogine, *From Being to Becoming*, San-Francisco: Freeman, 1979
- [15] W. Iskra and I. Rotter, *Phys. Rev C* 44, 721 (1991)
- [16] H.W. Barz, I. Rotter and J. Höhn, *Nucl. Phys. A* 275, 111 (1977)
- [17] C. Mahaux and H.A. Weidenmüller, *Shell Model Approach to Nuclear Reactions*, Amsterdam: North-Holland, 1969
- [18] I. Rotter, *Ann. Phys. (Leipzig)* 38, 221 (1981)

Figure 1

$Re\{\tilde{\gamma}_{Rc}^I\}$ for the inelastic neutron channel c_2 and for $\alpha^{ex} = .2$ to 8 (1a to 1h). The $\tilde{\gamma}_{Rc}^I$ for the two states $R = 1, 2$ with the largest widths are represented by dashed lines while the $\tilde{\gamma}_{Rc}^I$ of all the other states $R = 3, \dots, 70$ are shown by points at the radii r for which the calculations are performed. The solid curves belong to a typical trapped state.

Figure 2

$Re\{\tilde{\gamma}_{Rc}^I\}$ and $Im\{\tilde{\gamma}_{Rc}^I\}$ for the elastic channel c_1 (a,b,e,f) and the inelastic channel c_2 (c,d,g,h) in the case of proton decay. $\alpha^{ex} = .2$ and 8. The $\tilde{\gamma}_{Rc}^I$ for the two states $R = 1, 2$ with the largest widths are represented by dashed lines while the $\tilde{\gamma}_{Rc}^I$ of all the other states $R = 3, \dots, 70$ are shown by points at the radii r for which the calculations are performed.

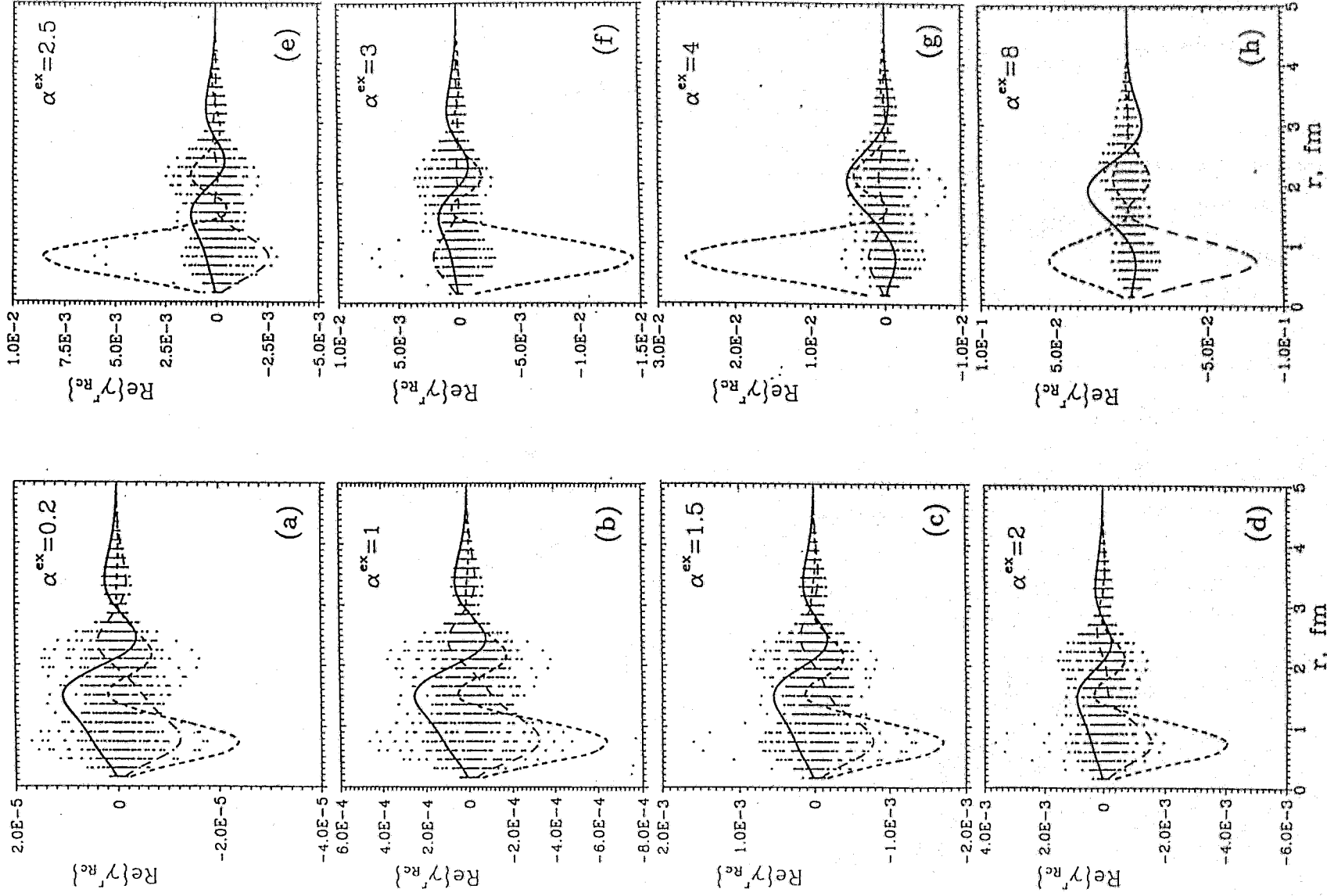


Figure 1

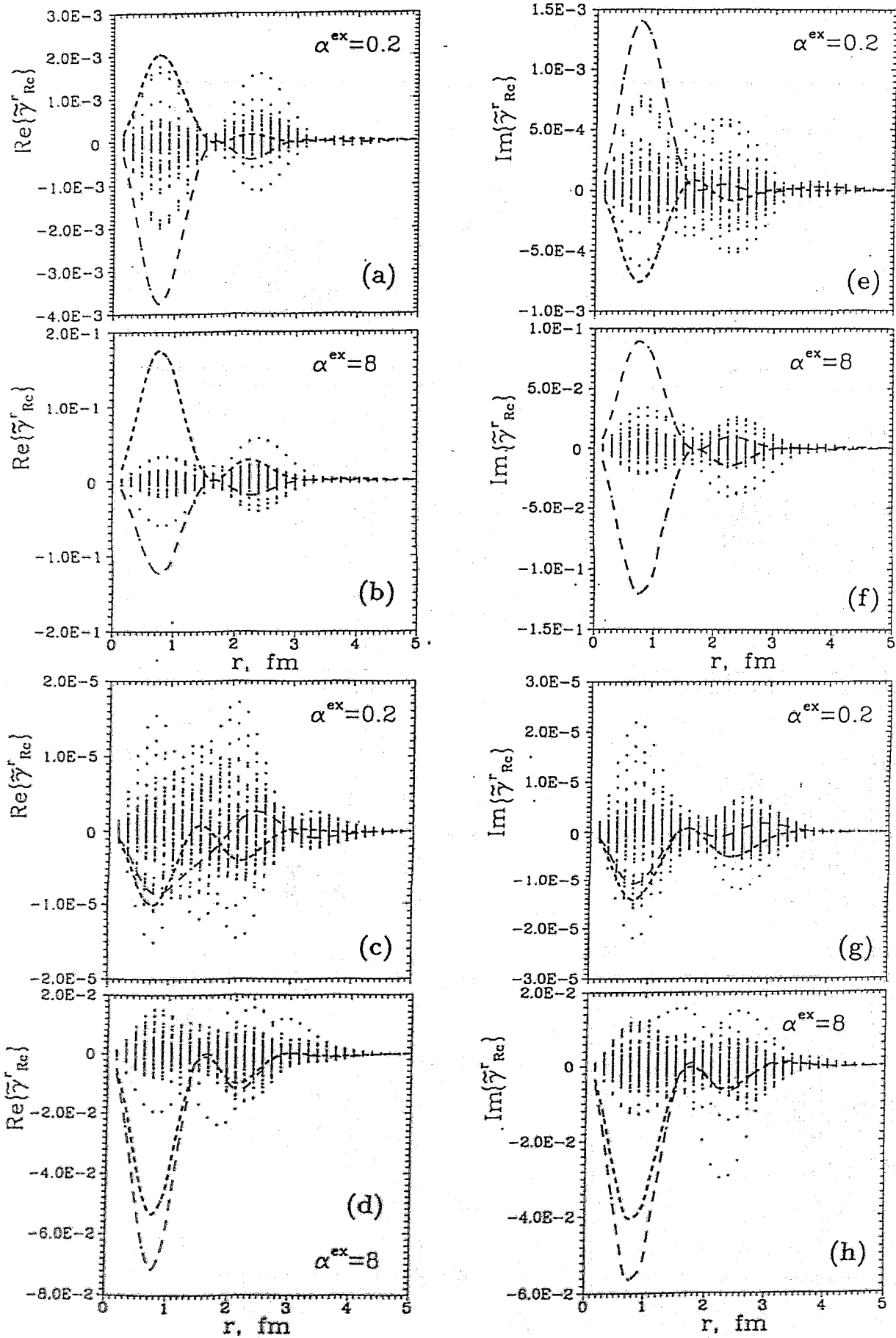


Figure 2